Touchscreen surface based on interaction of ultrasonic guided waves with a contact impedance

Nicolas Quaegebeur[a], Patrice Masson[a], Nicolas Beaudet[b], and Philippe Sarret[b]

[a]GAUS, Dept of Mechanical Engineering, Université de Sherbrooke, Sherbrooke, QC, J1K2R1
[b]IPS, Dept of Physiology and Biophysics, Université de Sherbrooke, Sherbrooke, QC, J1H5N4

ABSTRACT

In the present paper, a touchscreen device is proposed, based on guided wave reflection and transmission induced by the presence of an object. The principle uses the advantages of other acoustic waves devices in terms of simplicity and applicability to any thin surface but is not subject to classical drawbacks (single-touch, sensitivity to scratches or contaminant, impossibility to follow motion of contact point). The theoretical interaction of guided waves with a contact impedance are first derived in order to define the requirements of the sensor in terms of frequency range, mode, sensor type and location, and embedded electronics. Design criteria and experimental validation on a small prototype (300 x 300 mm) are proposed to demonstrate the potential of the approach for simple, robust and reliable contact detection and contact pressure estimation of point-like or extended objects for consumer electronics or biomedical applications.

Keywords: Touchscreen, Pressure sensor, Guided waves, Embedded electronics

1. INTRODUCTION

The popularity of smartphones, tablets, and many types of communication devices is driving the demand and acceptance of common touchscreens for portable and functional electronics.[1] In the medical field and in heavy industry, touchscreen devices are also widely used as replacement of keyboard and mouse systems for accurate interaction by the user with the displays content.[2] Amongst existing applications, touchscreen derivate products such as pressure mapping systems are also used in biomedical research in order to determine weight balance of humans or animals and determine the efficiency of a treatment during the clinical phase of drugs development.[3]

Three different technologies have been proposed since the 60's for touchscreen devices, namely electrical, optical and mechanical (acoustic) solutions.[2] Electrical solutions (capacitive and resistive) are widely used in consumer electronics for their flexibility of use but require expensive manufacturing in controlled environment since a matrix of transparent and conductive electrodes is inserted between two layers of glass or polymer.[4] Optical solutions (infrared or imaging) are more and more used for large screens and applications that require an extreme transparency. Those two technologies however do not allow measuring the contact pressure or extent and can only inform the user on the presence of contact point (single-touch or multi-touch).

In order to estimate the contact pressure, acoustic solutions must be envisioned. Surface Acoustic Waves (SAW) technology[5] uses high-frequency ultrasonic waves (above 1 MHz) by measuring the absorption of waves due to the presence of a contact. However, applications of SAW are very sensitive to contaminants on the surface (liquid, scratches) that produce false contact information. Moreover, multi-touch and extended contact cannot be taken into account, such that this technology is considered as obsolete. In the 2000's, acoustic pulse recognition[6] has been used to monitor acoustic impact sound (below 30 kHz) produced by a contact as in Acoustic Emission (AE). This technology allows using a reduced set of transducers (2 piezoceramics located at the corners) but is unable to monitor contact points after the initial touch, i.e. in the case of a motionless or sliding finger.

Further author information: (Send correspondence to Nicolas Quaegebeur)
E-mail: nicolas.quaegebeur@usherbrooke.ca, Telephone: 1 819 821 8000 # 61943

Industrial and Commercial Applications of Smart Structures Technologies 2017, edited by Dan J. Clingman,
Proc. of SPIE Vol. 10166, 101660F · © 2017 SPIE · CCC code: 0277-786X/17/$18 · doi: 10.1117/12.2258622

In the present study, a novel touchscreen device is proposed, based on ultrasonic guided wave reflection and transmission induced by the presence of an object. The approach uses the advantages of other acoustic waves devices in terms of simplicity and applicability to any thin surface but is not subject to classical drawbacks since it can follow the motion of contact point after the initial impact.

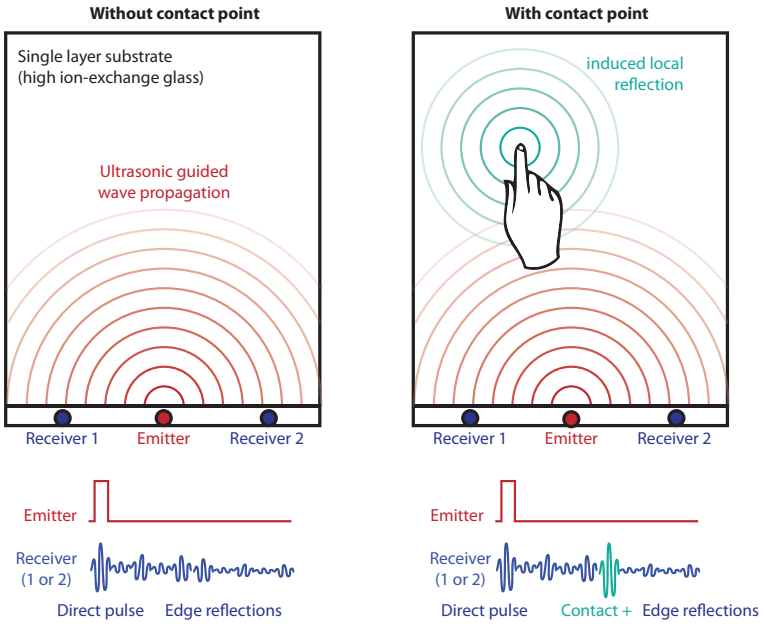

Figure 1. Principle of the touchscreen application based on guided wave interaction with an object in contact.

The principle of the sensor, described in Fig. 1, is to send an ultrasonic guided wave into a host structure and measure its response at different locations. In the absence of a contact, the reflections induced by the edges are observed. However, in the presence of a contact, local reflection is induced and modifies the measured vibration field. The idea is then to compare the measured response at the sensors with a database in order to retrieve the contact location and impedance value, since the reflection amplitude is directly related to the contact impedance.

The concept of using Lamb in an intermediate frequency range (20 - 500 kHz) waves instead of low frequency acoustic waves[6] or high frequency surface acoustic waves[5] has been first proposed[7] and patented by the authors.[8,9] In the same time, an equivalent system has also been patented.[10] The numerical modelling of the similar sensor can be found in[11] but the application to real-time contact detection has not been demonstrated so far. In the present paper, the analytical modelling, implementation of a dedicated electronic platform and demonstration of real-time contact imaging is proposed.

2. GUIDED WAVE INTERACTION WITH A CONTACT IMPEDANCE

2.1 Contact impedance modelling

A local contact on a thin structure of thickness $2h$ is responsible for two different effects. On the one hand, the object creates a local static deformation of the host structure which is highly related to the Young's modulus of both structures and the applied pressure. However, the local change of thickness corresponding to the inter-penetration distance is not important (few microns for normal use conditions), even on a very flexible structure.[12] In this case, the propagation of ultrasonic guided waves should not impaired by the change of thickness and no local reflection should be induced.

On the other hand, the local contact creates a local change of the surface stress field, such that the propagation of guided waves is locally modified. The contact applied over a surface ΔS can be described as a local contact

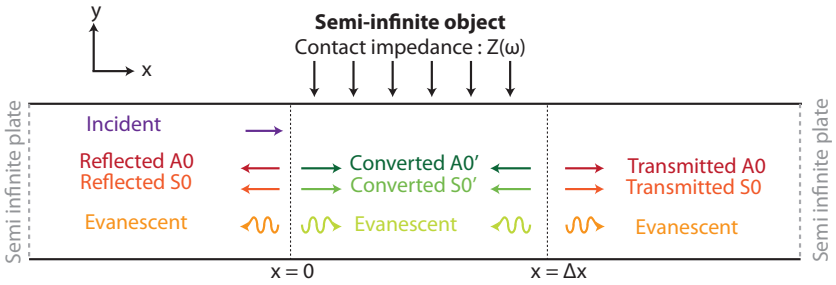

Figure 2. Scheme of the considered geometry for calculation of reflection and transmission induced by an contact impedance of a finite dimension Δx.

impedance matrix $Z(\omega)$ as described in Fig. 2. In the present paper, the contact with small objects (pencil, finger, animal paw) on a thin structure is considered, such that the applied pressure at the contact can be neglected. Under this assumption, non diagonal terms of the impedance matrix can be neglected and the contact impedance matrix can be considered diagonal and the diagonal terms are both equal to the normal surface contact impedance $Z_n(\omega)$ that is classically modelled as a mass M, a normal contact stiffness term K and a contact damping factor ξ:

$$Z_n(\omega) = \frac{M\omega^2 - K(1+j\xi)}{j\omega\Delta S} \tag{1}$$

In the present paper, the influence of added impedance on the guided wave propagation is first studied in order to characterize the induced reflection and transmission coefficients. In the following sections, the term $Z_n(\omega)$ is chosen as a pure negative imaginary term, representing an added mass only and thus neglecting the stiffness and damping effects of the contact for clarity, since in the case of a fingertip, only the mass effect is observed above 1 kHz.[13]

2.2 Reflection and transmission in the presence of a contact impedance

As presented in,[7] the influence of the contact impedance can be non-dimensionalized by considering the coefficient Γ defined as follows:

$$\Gamma(\omega) = \frac{j\omega Z_n(\omega)}{\mu} \approx \frac{M\omega^2}{\mu} \tag{2}$$

where μ denotes the Lam coefficient. In this section, the calculation of reflection and transmission induced by the contact impedance $Z_n(\omega)$ is considered in the case of a semi-infinite contact region. In order to derive the reflected and transmitted coefficients, the continuity of in-plane $u_x(0,y)$ and out-of-plane $u_y(0,y)$ displacement fields evaluated at $x = 0$ is considered, as classically proposed in.[7,14]

In Fig. 3, it appears that mode reflection is strongly dependent on the applied contact impedance and frequency but the same tendencies are observed independently on the considered incident mode. As mentioned previously, high values of parameter Γ correspond to a quasi-clamping condition and lead to a quasi perfect reflection of the incident mode (A_0 or S_0 modes). The transition between no reflection and perfect reflection is observed between $\Gamma = 10$ and $\Gamma = 10000$ depending on the frequency. Mode conversion also increases with respect to frequency but is limited (3% and 1.5 % for A_0 and S_0 incident mode respectively) and not presented here for clarity.

3. IMPLEMENTATION FOR CONTACT DETECTION AND LOCALIZATION

3.1 Contact detection and localization

In order to retrieve information on the contact location and applied contact impedance, an imaging procedure is required. The principle is to divide the sensitive surface into a grid of observation points and to determine the

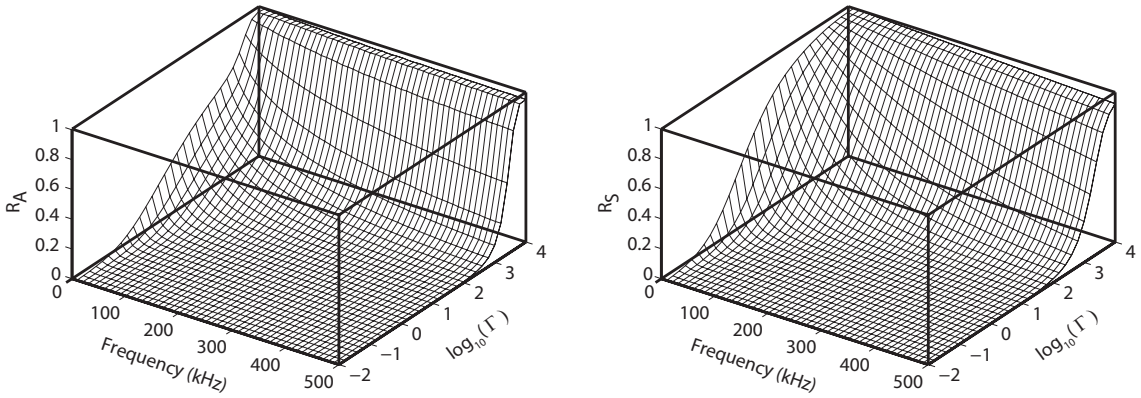

Figure 3. Reflection coefficients in the case of incident A_0 mode (left) or S_0 mode (right) as a function of non-dimensionalized contact impedance Γ and frequency.

probability of presence of a contact point at each of the points of the grid. Common imaging algorithms used with guided waves are based on Time-of-Flight (ToF) analysis of the reflected wave, such as Delay-and-Sum,[15] assuming a simple non dispersive single-mode propagation. Recently, a correlation-based method has been proposed for Structural Health Monitoring[16] or Non-Destructive Testing,[17] allowing to take into account dispersive and multi-mode propagation, transducers coupling and complex interactions with reflectors.

However, this model-based imaging algorithms assumes that the structure, edge reflections and transducer dynamics can be accurately modelled. In order to reduce the localization errors and take into account the dedicated electronics, an experimental database is used instead. For this purpose, an automated test bench has been developed in order to apply a calibrated contact impedance to different points of the structure. This allows constructing the signal database that contains the contact signature over a given grid of observation point. In the present case, a grid of 150 x 150 points for a precision of 2 mm in the contact imaging is used. For a given design (electronics, host structure, transducers), this signal database is required once and can be done with a resolution up to 0.5 mm.

Once the database is constructed, the correlation between the signals in the database and the measured signals is performed using a Generalized Cross-Correlation (GCC) formalism[18] that allows performing the correlation in a given frequency range. This method is a generalization of the cross-correlation in the frequency domain that allows compensating for dispersive propagation, multiple reflections in reverberant spaces and moderate background noise conditions.[19] Thus, the imaging result $I(x, y)$ at pixel (x, y) can be expressed as the summation of contribution of the N transducers as follows:

$$I(x,y) = \frac{1}{N}\sum_{i=1}^{N}\int_{f_1}^{f_2} W(f)\mathcal{M}_i(f)\mathcal{D}_i(x,y,f)df \tag{3}$$

where f_1 and f_2 represent the lower and upper frequency bounds defined by the material selection and application requirements as described in the following section, $\mathcal{M}_i(f)$ represents the Fourier transform of the measured signal at the transducer i, $\mathcal{D}_i(x, y, f)$ denotes the Fourier transform of the database signal at pixel (x, y) and transducer i, and $W(f)$ is a frequency weighting function used in the GCC formalism. In order to determine the contact pressure, the normalization has to be adapted and a new frequency windowing is introduced as follows:

$$W(f) = \frac{1}{|\mathcal{D}_i(x,y,f)|\int_{f_1}^{f_2}|\mathcal{D}_i(x,y,f)|df} \tag{4}$$

3.2 Material and transducers selection

Considering that the application requires transparency, only polymers or glass could be used. Moreover, in order to achieve high sensitivity to small contact pressure, the Lam coefficient μ should be selected as low as possible,

while keeping the damping ratio (loss factor) as low as possible. For this reason, a 0.5 mm polycarbonate film sheet has been selected. For a biomedical application, masses in the range of 1 to 100 g are considered for a contact area smaller than 10 mm x 10 mm (typical rodent paw contact area), corresponding to a local pressure of approximatively 0.1 to 10 kPa. As described in Fig. 3, the guided wave reflection occurs for $100 < \Gamma < 10000$. In order to get maximal reflection for the maximal mass and no reflection for the minimal mass, the frequency range is derived combining Eqs. 1 and 2. For the considered glass plate, the optimal frequency range would thus be 20-80 kHz, representing a wavelength range of 15 - 2 mm for A_0 mode. This frequency range is thus used for computation of the correlation coefficient described in Eq. 3, allowing discarding the contribution from background vibration in the audible range.

Piezoceramic transducers are used for generation and sensing of guided waves due to their small footprint, low cost, high temperature stability and ease of use. The transducer size selection is based on mode-tuning for desired wavelength.[20] Since the precision of the imaging technique is partially related to the wavelength, A_0 mode is selected. In the present case, a standard 5 mm diameter piezoceramic can be used in order to maximise the energy transferred to the glass plate around 80 kHz. In the present application, 8 piezoceramics are used (4 actuators plugged in parallel and 4 sensors) and placed at the edge of the considered sheet in order to minimize the total footprint of the transducers and maximize the detection area, as presented in Figs. 1 and 4.

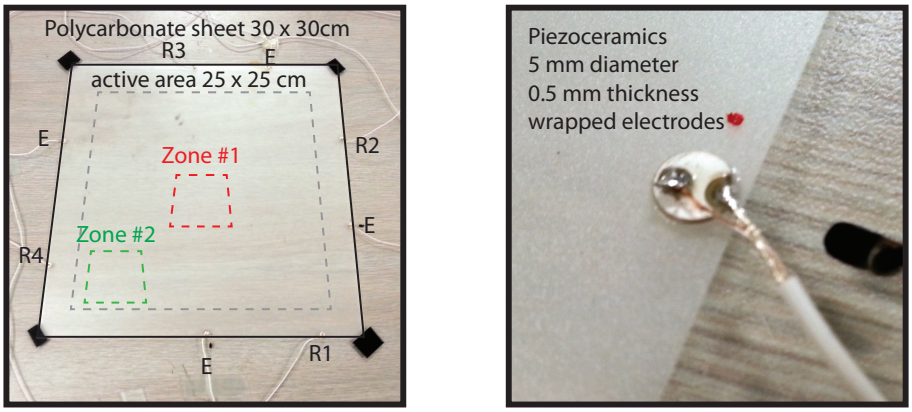

Figure 4. Photography of the 300 x 300 mm prototype (left) and zoom on a piezoceramics (right).

3.3 Embedded electronics

For this purpose, a dedicated electronic platform has been developed in collaboration with UNGAVA Tech. The platform includes a high voltage pulser (100 V peak) for the actuator, 3 parallel ADC lines for acquisition at 10 MHz and the imaging process is handled by a Zynq Z-7010 composed of a FPGA and an ARM Cortex 9 embedded in a single chip with shared memory, allowing to split the tasks between both parts of the micro-processor. For instance, the acquisition of 1 ms, averaging of 10 repetitions and Fast Fourier Transform is performed on the FPGA side while the correlation, contact imaging and host PC communication are implemented on the ARM for simplicity.

Considering a 150 x 150 grid, the correlation is executed in the frequency domain using GCC formalism, as described in the previous section. Real-time correlation of the measurement with the whole database signals is achieved in approximatively 30 ms, such that real-time imaging is obtained. Imaging results are then transmitted to a host PC using a USB 2.0 connection and display is performed on a screen underneath the touchscreen.

4. EXPERIMENTAL ASSESSMENT

4.1 Contact localization

The validation in the case of point-like contact is performed using a circular mass of 25 g and 10 mm diameter. Fig. 5 presents the imaging results over the whole touchscreen in the case of two zones as presented in Fig. 4. In

all cases, only a zoom around the regions of interest (30 x 30 mm) is presented in order to describe the precision and spatial extent of the imaging.

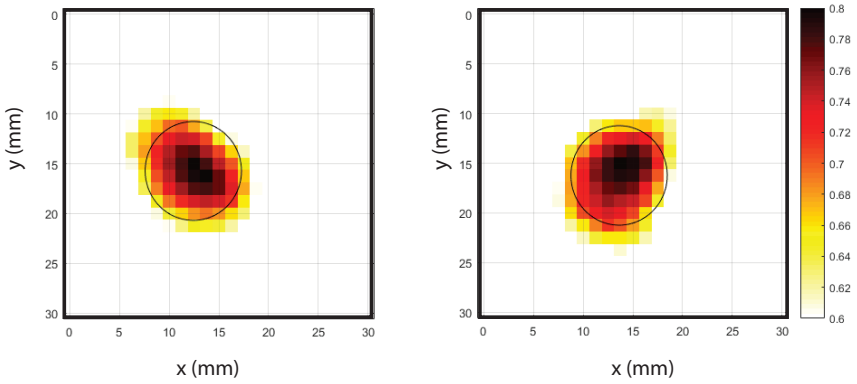

Figure 5. Imaging for a 10 mm diameter contact at two different locations.

In Fig. 5, it appears that a very precise localization of the contact point is achieved in both cases, and more generally, single contact localization without any drift is observed on the whole surface, even at the edges of the plate. The imaging over the whole area exhibits no false positive using a fixed threshold.

4.2 Sensitivity

In order to characterize the sensitivity of the proposed method, the measured correlation coefficient using Eq. 3 is estimated for different contact pressures and presented in Fig. 6.

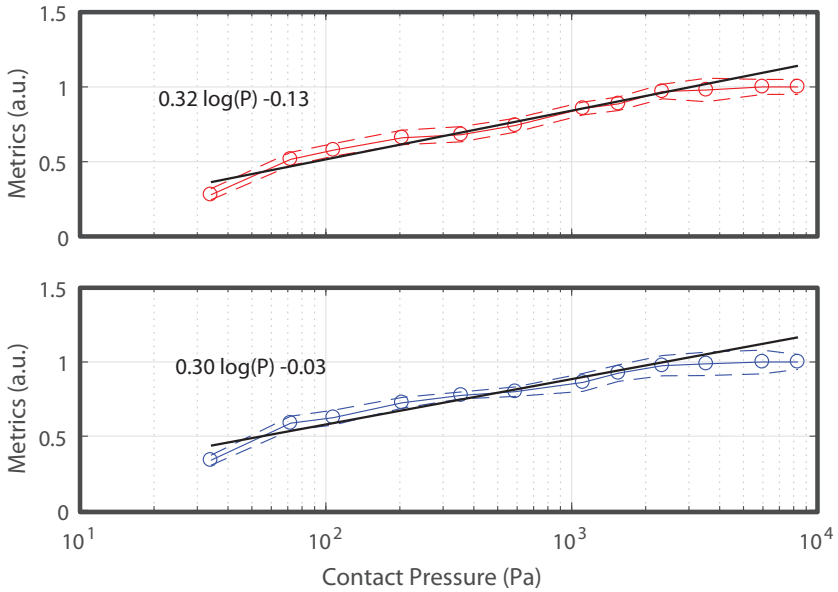

Figure 6. Sensitivity analysis at the zone 1 (top) and zone 2 (bottom).

In Fig. 6, it appears that a linear tendency is observed for the metrics as a function of the log of the contact pressure. This tendency is in accordance with the observations of Fig. 3 that suggest a linear behavior for Γ between 10 and 10000, while a saturation effect occurs above 10000, corresponding to approximatively 2 kPa in the present case. Below 30 Pa, the background noise impairs the measurement and limit the sensitivity of the

sensor. However, this value is relatively small and corresponds to 250 mg distributed over a circle of 10 mm diameter. The sensitivity analysis at two locations is presented here in order to demonstrate the independence with respect to the contact location. Indeed, the linear tendency has approximatively the same slope at the two locations and only a small variation of the metrics obtained at 1 Pa is observed.

4.3 Repeatability

In order to assess the drift and repeatability of the method, the extraction of the contact pressure as a function of time is performed at a sampling frequency of 100 Hz. Results of the drift and repeatability are presented in Fig. 7.

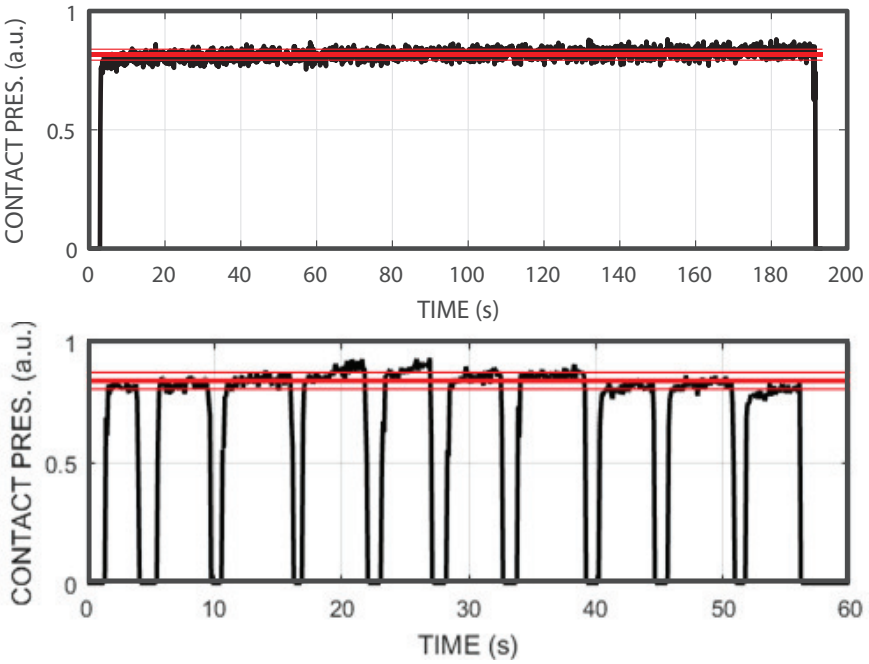

Figure 7. Drift over a long time (top) and repeatability over 10 measurements (bottom) in the case of a 25 g mass.

In Fig.7, it appears that a negligible drift can be observed over a 3 min period, with a small increase of 0.9 % per minute. The observed variability (standard deviation) over this period is around 2.5 % over the 180000 samples. Looking at the results of repeatability in the case of multiple repetitions, a small deviation of 5 % is observed over the whole acquisition time.

5. CONCLUSION

In the present paper, a novel contact pressure sensor is proposed, based on guided wave reflection induced by the presence of an object. The principle uses the advantages of other acoustic waves devices in terms of simplicity and applicability to any thin surface but is not subject to classical drawbacks (single-touch, sensitivity to scratches or contaminant, impossibility to follow motion of contact point). Design criteria and experimental validation on a small prototype (300 x 300 mm) are proposed and demonstrate the potential of the approach for simple, robust and reliable touchscreen applications for consumer electronics or biomedical applications.

Acknowledgments

The authors would like to thank the Institute of Pharmacology of Sherbrooke (IPS), the Interdisciplinary Institute for Technological Innovation (3IT), the Canadian Arthritis Network (CAN) and the Natural Sciences and Engineering Research Council of Canada (NSERC) for their financial support. Many thanks to Emmanuel Lizé and Louis-Philippe Brault for their support during the experimental part of the work.

REFERENCES

[1] Dai, J. and Chung, C.-K., "Touchscreen everywhere: On transferring a normal planar surface to a touch-sensitive display," *Cybernetics, IEEE Transactions on* **44**, 1383–1396 (Aug 2014).

[2] Holzinger, A., "Finger instead of mouse: touch screens as a means of enhancing universal access," *Universal Access Theoretical Perspectives, Practice, and Experience* **1**, 387–397 (2003).

[3] Rashid, M., Theberge, Y., Elmes, S., Perkins, M., and McIntosh, F., "Pharmacological validation of early and late phase of rat mono-iodoacetate model using the Tekscan system," *European Journal of Pain* **1**, 1–6 (2012).

[4] Lee, J., Cole, M., Lai, J., and Nathan, A., "An analysis of electrode patterns in capacitive touch screen panels," *Display Technology, Journal of* **10**, 362–366 (May 2014).

[5] Adler, R. and Desmares, P., "An economical touch panel using SAW absorption," *IEEE transactions on ultrasonics, ferroelectrics, and frequency control* **34**(2), 195–201 (1987).

[6] Kiri, R., Quieffin, N., Catheline, S., and Fink, M., "In solid localization of finger impacts using acoustic time-reversal process," *Applied Physics Letters* **87**(20), 204104–204104 (2005).

[7] Quaegebeur, N., Masson, P., Beaudet, N., and Sarret, P., "Touchscreen surface based on interaction of ultrasonic guided waves with a contact impedance," *IEEE Sensors Journal* **16**, 3564–3571 (May 2016).

[8] Quaegebeur, N., Masson, P., Beaudet, N., and Sarret, P., "Pressure mapping system based on guided waves reflection," in [*Proceedings of Meetings on Acoustics*], **19**(1), 030110, Acoustical Society of America (2013).

[9] Masson, P., Quaegebeur, N., Ostiguy, P.-c., Beaudet, N., and Sarret, P., "Active acoustic pressure mapping system," (July 2015).

[10] Khuri-yakub, B. T., Nikoozadeh, A., and Firouzi, K., "multi-touch ultrasonic touch screen," (October 2015).

[11] Firouzi, K., Nikoozadeh, A., and Khuri-Yakub, B., "Numerical modeling of ultrasonic touchscreen," in [*Ultrasonics Symposium (IUS), 2014 IEEE International*], 753–756 (Sept 2014).

[12] Johnson, K. L., [*Contact mechanics*], Cambridge university press (1987).

[13] Wiertlewski, M. and Hayward, V., "Mechanical behavior of the fingertip in the range of frequencies and displacements relevant to touch," *Journal of Biomechanics* **45**(11), 1869 – 1874 (2012).

[14] Rokhlin, S. I., "Lamb wave interaction with lap-shear adhesive joints: Theory and experiment," *The Journal of the Acoustical Society of America* **89**(6), 2758–2765 (1991).

[15] Giurgiutiu, V., Zagrai, A., and Bao, J., "Piezoelectric wafer embedded active sensors for aging aircraft structural health monitoring," *Structural Health Monitoring* **1**(1), 41–61 (2002).

[16] Quaegebeur, N., Masson, P., Langlois-Demers, D., and Micheau, P., "Dispersion-based imaging for structural health monitoring using sparse and compact arrays," *Smart Materials and Structures* **20**(2), 1–10 (2011).

[17] Quaegebeur, N. and Masson, P., "Correlation-based imaging technique using ultrasonic transmit?receive array for non-destructive evaluation," *Ultrasonics* **52**(8), 1056 – 1064 (2012).

[18] Knapp, C. and Carter, G. C., "The generalized correlation method for estimation of time delay," *Acoustics, Speech and Signal Processing, IEEE Transactions on* **24**(4), 320–327 (1976).

[19] Quaegebeur, N., Padois, T., Gauthier, P.-A., and Masson, P., "Enhancement of time-domain acoustic imaging based on generalized cross-correlation and spatial weighting," *Mechanical Systems and Signal Processing* **75**, 515 – 524 (2016).

[20] Raghavan, A. and Cesnik, C., "Finite-dimensional piezoelectric transducer modeling for guided wave based structural health monitoring," *Smart Materials And Structures* **14**, 1448–1461 (2005).